Long-Term Behavior of Large-Span Culverts in Cohesive Soils

M. C. McVay, P. Papadopoulos, D. Bloomquist, and F. C. Townsend

The long-term (after end of construction) behavior of large-span culverts buried in cohesive soils is presented. Nine centrifuge tests encompassing three different culvert shapes and three soils of varying degrees of plasticity were conducted. Backfill depth over the crown was fixed at 4.8 m to minimize the effect of vehicular live loads and to represent field conditions. The results show that the culvert's original shape controls its deformed shape and possible failure mode. For instance, the crowns of the semicircular culverts were rising, whereas the crowns of the low-profile arches were subsiding. The soil's plasticity was related to the magnitude of stress and deformation increase, and a linear relationship between bending moment and soil plasticity was discovered. In general, axial stress increases of 10 to 50 percent and bending moment increases of 50 to 100 percent, depending on soil plasticity, were recorded. It is suggested that long-term stress changes be accounted for in the future design of cohesive soils.

As small bridges and grade crossings have become old and in need of replacement, alternatives such as large-span steel or aluminum culverts have become economical substitutes for the more traditional bridge deck structures. Among the reasons for their increased use are simplicity of construction (may use unskilled labor), shorter installation times, minimum foundations requirements, and lower costs of construction materials. Typically assembled of corrugated metal plates of wall thicknesses varying from 0.25 to 1.25 cm, the complete structure may have a span (diameter) of 4 to 15 m and a backfill cover ranging from a few meters to 100 m (*1*).

The present AASHTO design (*2*) considers dead and live loads in sizing the plate. Special features such as thrust beams to promote arching and rib stiffeners to increase the cross-sectional moment of inertia of the section are also required. A select granular fill (Unified Soil Classification, GW), compacted to 90 percent AASHTO T180, extending 1.8 m from the side and 1.2 m above the structure, is compulsory. The code does not prohibit the use of cohesive (plastic) borrow soil as embankment material around the granular zone. This material is generally used if granular soils are unavailable on the site for economical reasons.

Long-term movements of the structure have been noted at a number of sites. Deflection increases on the order of 50 percent (*3*) and even catastrophic failures (*4*) have been recorded after a number of years. Currently the four most commonly cited causes of long-term soil-culvert stress and deflection reapportionment (*5*) are time rate consolidation, secondary compression, dynamic vehicular loads, and seasonal temperature and moisture variations associated with the environment.

Department of Civil Engineering, University of Florida, 345 Weil Hall, Gainesville, Fla. 32611.

The objective of the research reported here was to determine the influence of culvert shape (geometry) and soil plasticity on the long-term stresses and deflections within the structure due to consolidation. The study was performed in a large [117-cm (46-in.) radius] geotechnical centrifuge. It has been shown (*6*) that by properly modeling the construction sequence, soil type, and structural geometry, the end of construction and the long-term response of the prototype soil-culvert system can be simulated. Combinations of three frequently used culvert sections with three ranges of soil plasticity (plasticity indexes of 6 percent, 16 percent, and 31 percent) were investigated for a total of nine cases. The height of backfill over the crown (top) was constant (5 m) and was obtained from median field values reported in the literature. All culverts were instrumented with strain gauges and linear variable differential transformers (LVDTs) to measure deformation, a grid of sequins to measure soil deformation, and a pore pressure transducer to monitor the clay's fluid pressures.

Results of the experiments reveal that the culvert's initial shape controls both the end of construction as well as the long-term deformation of the structure. The soil type controlled the magnitude of both the long-term thrust and the bending stresses. Ring compression theory (*2*) can predict very well the thrust stress in the culvert wall at end of construction. However, depending on soil type, increases on the order of 50 percent may develop in the long term for very plastic soils. A linear relationship was found between bending stress and the plasticity index. The latter is important in estimating collapse, that is, the formation of plastic hinges.

LABORATORY EQUIPMENT AND MATERIALS

The containment vessel used to house the soil-culvert model in the centrifuge is shown in Figure 1. The inside dimensions of the container are 25.4 by 30.5 by 25.4 cm deep. The size ensured that the acceleration field within the bucket did not vary by more than 10 percent. The four walls of the box are 2.54-cm-thick Plexiglass and covered with an indelible 1.25- by 1.25-cm grid for determining soil strains using Avgherinos' photographic technique (*7*). The bottom of the container is removable, facilitating the placement of the culvert and instrumentation. The top of the bucket was slotted for the use of the inflight soil compactor (*6*).

The three long spans studied were the low-profile, semicircular, and high-profile arches because they are the most

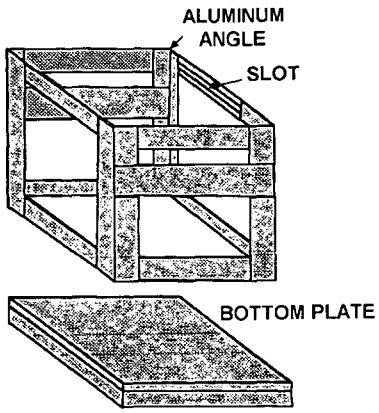

FIGURE 1 Containment vessel housing soil-conduit system.

commonly used shapes. The low-profile and high-profile arches have a larger radius of curvature at the crown than the semicircular shape and a smaller one from the thrust beams to the springline (side). The high-profile arch differs from the low profile arch in that the angle subtended in the former is much greater than that of the latter.

The clay backfill was selected to provide a large variability in terms of compressibility and permeability. Table 1 presents the properties of the three soils used and their classification. The compressibility of the green clay is greater than that of the red clay, which is greater than that of the orange clay; the permeability of the orange is greater than that of the red clay, which is greater than that of the green clay. All clay backfill was placed at optimum moisture content (Table 1) and compacted in flight (*6*).

The depth of backfill over the crown (top) of the culvert was selected to minimize the influence of vehicular loading and yet characterize a typical site. From a literature review, a total backfill depth of 4.8 m was selected. The AASHTO (*2*) specifications stipulate a granular zone of fill, 0.7 m above and 1.8 m alongside the culvert. Figure 2 shows the three prototype structures and backfill depths. All three culverts had the same depth of backfill over the crown because the study was concerned with only the influence of culvert geometry and soil type.

The centrifuge tests were conducted at the maximum *g*-level that would limit the stress variation within the bucket (Figure 1) to 10 percent (55 *g*'s). All three culvert models were made from 0.64-mm-thick aluminum plate and cold rolled. The wall thickness was selected from similitude of bending stiffness (EI/C, where E = Young's modulus, I = moment of inertia, and C = distance from neutral axis to outside fiber) between models and the suggested AASHTO design (15.2- by 5.1-cm corrugations with 0.55 wall thickness). Table 2 provides the complete model geometries for the three structures (Figure 2) under study.

Each model had pairs of strain gauges epoxied to the inside and outside of the culvert at its springline, thrust beam, and crown locations. For redundancy, wear, and tear, each location had three sets of strain gauges for a total of 18 gauges on each model. For a given pair (inside and outside), the average strain may be equated to the thrust stress, and the average of the difference to the bending stress in the wall.

Deformations of the crown of the culverts were determined using an LVDT and subsequently converted to prototype movements by multiplying them by the *g*-level of the test (55 *g*). Figure 3 shows an instrumented model culvert with the AASHTO (*2*) special feature, that is, thrust beams.

The soil was instrumented with a Druck miniature 1-bar (100-kPa) PDCR–81 pore pressure transducer. McVay et al. successfully used a similar device (*6*) to measure pore pressures at different scale sizes to confirm the pore pressure dissipation was *g*-level squared, that is, classical consolidation theory. The transducer was placed 4.1 cm outward from the springline in the clay backfill. To measure soil strains, straight pins with flat heads were placed with each soil lift, touching the grid-lined Plexiglass. A Swiss Kern DSR–1 device, which is accurate to 1 micron, was used to measure the relative movements of the markings.

TEST RESULTS

Deflections

The deflections of the three culverts versus model time with different backfill types are shown in Figure 4. Model time may be converted to prototype time by multiplying it by $(55)^2$, which is the scaling relationship for viscous consolidation time (*6*). In Figure 4, time zero represents no backfill (i.e., start of construction) followed by the end of construction (EOC) (20-min model or 42-day prototype time) and afterwards for a total of 320 min (1.8-year prototype). All structures experienced crown peaking at 10 min (21-day prototype) because backfilling reached the culvert's crown at this point, followed by subsidence as backfilling occurred from the crown (10-min

TABLE 1 Clay Backfill Properties

	Low Plasticity Orange Clay	Med. Plasticity Red Clay	High Plasticity Green Clay
Maximum Dry Density (kN/m^3)	18.69	17.28	12.72
Optimum Moisture Content	13%	21%	36%
Liquid Limit	21%	33%	71%
Plasticity Index	6%	16%	31%
Classification*	CL-ML	CL	MH

* Based on Unified Soil Classification System

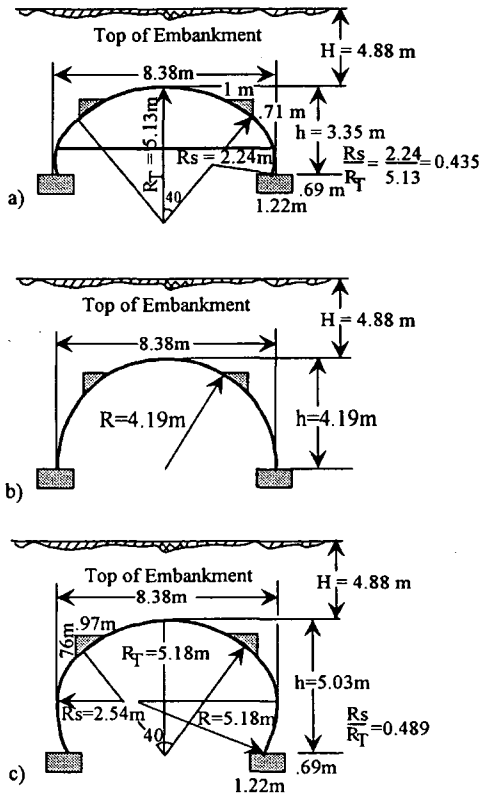

FIGURE 2 Culvert geometries and backfill depths: (*a*) low-profile arch; (*b*) semicircular arch; (*c*) high-profile arch.

model) to its final depth, that is, EOC (20-min model or 42-day prototype time).

As expected, the order of crown peaking due to depth of backfill at the crown after the 10-min mark (21-day prototype) was the high profile, then the semicircle, followed by the low-profile arch. Also, for a given shape, the crown peaking appears to be influenced by the soil's plasticity (Figure 4). The latter may be explained from the compaction induced stresses which, according to Duncan and Seed (*8*), approach passive values. For shallow depths, the passive pressure is controlled more by the soil's cohesion than its angle of internal friction. For instance, Table 3, which presents the resultant passive force (Pp1) on the low-profile arch, shows the high-plasticity green clay to have the greatest passive force. Consequently, a structure will tend to flex inward to a larger extent when interacting with a very plastic soil (higher cohesion) than with a less cohesive soil. All three structures displayed this phenomenon.

Backfilling over the crown (10 min) to the end of construction (20 min) resulted in crown subsidence from overburden weight. Also, the more plastic the clay, the more the subsidence. The latter is due to the lower passive resistance for the green clay compared to its orange counterpart. Because for moderate depths and deeper, Rankine passive pressure coefficient (Kp) times depth (z) is more significant than the cohesion term. Table 3 presents the resultant passive force (Pp2) on the side of the low-profile culvert at the end of construction for all three clays.

Displacement of the structures from EOC onward is due to the long-term dissipation of excess pore water pressures (consolidation). As expected, the low- and high-profile arches displaced downward due to the consolidation of the clay soil alongside the culvert. However, the semicircular arch's crown moved upward. This unexpected result may be explained from its shape at EOC as shown in Figure 5(*b*) for the high-plasticity clay. Clearly displayed is the concave outward curvature at its thrust beam (shoulder) location compared to the inward curvature of the other structures [Figures 5(*a*) and 5(*c*)] at EOC. From the end of construction onward (long term), these curvature changes are accentuated as shown in Figure 5 for all structures. The long-term consolidation deformations of the high-plasticity clays around the semicircular arch support these findings (Figure 6). The structure is moving inward more at its shoulder than outward at its springline, resulting in the crown rising.

These results agree very well with the long-term failure of a semicircular arch reported in *Engineering News Record* (*4*), in which it was stated that the crown was rising and the shoulders (thrust beam) were subsiding just before failure.

It should be noted that the semicircular arch was the only structure studied that did not have a reentrant angle at its footing. One way to alleviate the semicircular's outward curvature at its shoulder is to use a reentrant angle at its footing (i.e., instead of 180 degrees, use 200 degrees as in a horseshoe arch). The latter would ensure an increase in the inward curvature at the structure's shoulder when backfilling from the footing to its springline (*9*).

TABLE 2 Model Geometries

Culvert	Low Profile	High Profile	Semicircular
Culvert Wall Thickness	0.64 mm	0.64 mm	0.64 mm
Culvert Width (span)	15.2 cm	15.2 cm	15.2 cm
Culvert Height	6.1 cm	9.1 cm	7.6 cm
Height of Fill over Crown	8.9 cm	8.9 cm	8.9 cm
Total Height of Clay Backfill	15.0 cm	18.0 cm	16.5 cm
Height of Granular Fill over Crown	1.3 cm	1.3 cm	1.3 cm
Width of Granular Fill at Springline	3.3 cm	3.3 cm	3.3 cm

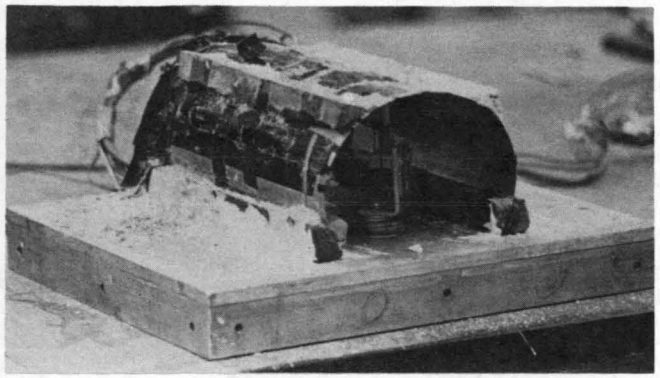

FIGURE 3 Model culvert with attached strain gauges and LVDT.

Stresses

Figure 7(*a*) shows the measured pore pressure in the orange (low plasticity) clay backfill near the springline of the low- and high-profile culverts from the end of construction onward. The decrease in pore water pressure to a constant value (hydrostatic) with time is evident and confirms the consolidation process. Also shown is an estimate of the hydrostatic pore pressure within the clay deposit at the location of the pore pressure transducer. The rise in its value with time is due to the decrease in the clay's void ratio as a result of the consolidation process. The measured pore pressure in the high-profile culvert's backfill starts and ends with higher values than the low-profile value due to its deeper clay deposit (Table 2). Consolidation effects appear to end within 100 min of model time or 210 prototype days.

Figure 7(*b*) shows the measured pore pressure in the red (medium plasticity) clay backfill near the springline of the semicircular and low-profile arches from the end of construction onward. Clearly depicted is a rise in pore pressure and then a decay toward a steady-state hydrostatic value. This rise is believed to be positive arching in which load (overburden weight above culvert) is being transferred to the clay backfill alongside the culvert's springline. This behavior was substantiated by the thrust stresses.

Shown in Figure 7(*c*) is the recorded pore pressures for the green highly plastic clay at the springline of the semicircular and high profile arches. Note the gradual rise and subsequent flattening of the curves. The rise follows the increase in hydrostatic pore pressure (as shown estimated in Figure 7(*c*)) due to a diminishing void ratio (consolidation). The largest excess pore water pressure occurs at the end of construction, suggesting that no arching is occurring. As expected, the higher the plasticity, the greater the amount of time required for dissipation (consolidation) to occur due to the soil's lower permeability.

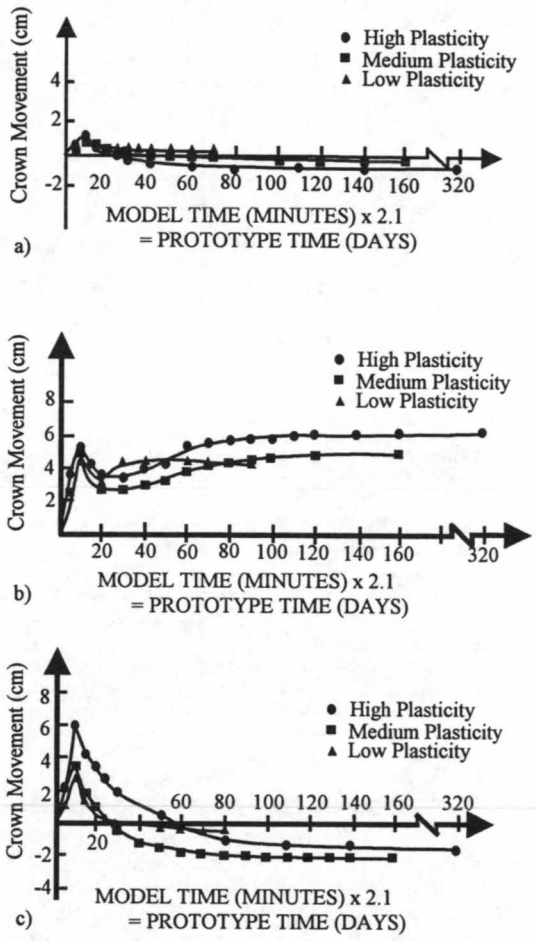

FIGURE 4 Deflection of top of culverts from beginning of construction onward: (*a*) low-profile arch; (*b*) semicircular arch; (*c*) high-profile arch.

Table 4 provides the ratios of the measured EOC and long-term (LT) thrust stresses in the wall of the culverts at their

TABLE 3 Passive Pressures

	ϕ	C (kPa)	γ (kN/m^3)	Kp	At Crown Pp1 (kN/m)	EOC Pp2 (kN/m)
Low Plasticity	38	4.79	21.49	4.20	316.33	1169.61
Medium Plasticity	34	14.36	19.85	3.54	340.31	1097.87
High Plasticity	25	28.73	19.92	2.46	365.90	1023.72

where $Pp = \int_o^H (2C\sqrt{Kp} + \gamma z Kp)\, dz$

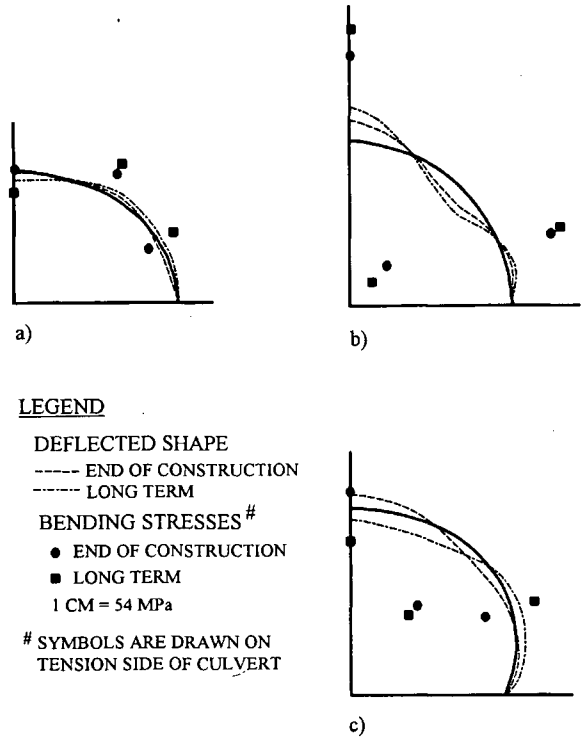

FIGURE 5 Deflected shape and bending moments in culverts: (*a*) low-profile arch; (*b*) semicircular arch; (*c*) high-profile arch.

springlines versus computed values from White and Layer (WL) (*10*) and AASHTO (*2*). White and Layer's thrust stresses are computed by multiplying the unit weight of overburden soil by the depth of fill above the culvert's crown by the culvert span divided by two. In the case of AASHTO, the thrust stress equation is the same as that of White and Layer, except that the span is replaced with twice the top arch radius of the culvert. Figure 8 plots the ratio of LT thrust stresses to those predicted by WL and the AASHTO code (AC) given in Table 4.

As is evident from Table 4, White and Layer's theory predicts very well the thrust stresses at the end of construction (all within 20 percent) and is usually conservative. The AASHTO code is more conservative (25 to 30 percent) for

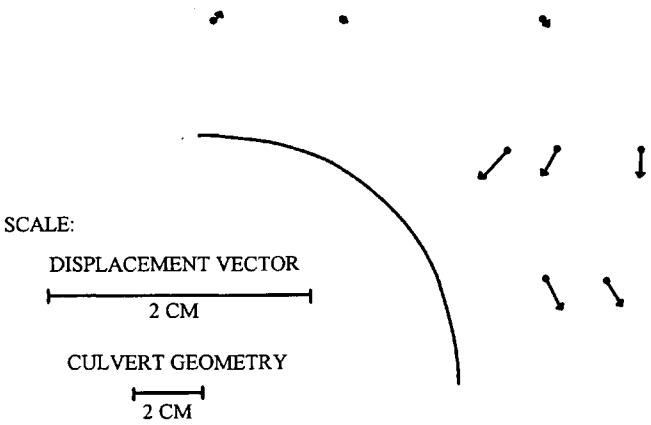

FIGURE 6 Long-term deformations in green backfill clay.

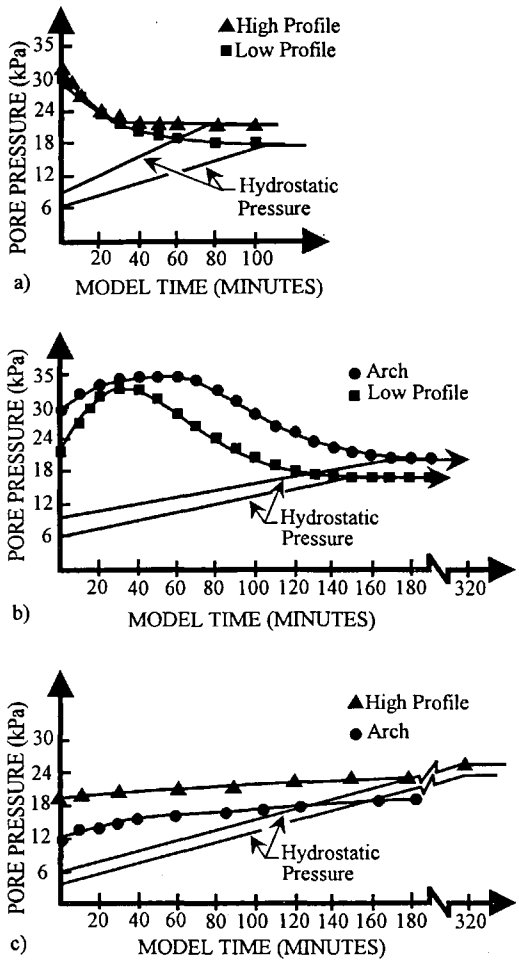

FIGURE 7 Pore water pressure at culvert springline: (*a*) low-plasticity clay; (*b*) medium-plasticity clay; (*c*) high-plasticity clay.

the low- and high-profile culverts at end of construction. Both gave the same result for the semicircular arch (unconservative ≈ 20 percent) because they both use the same radius and/or span of the structure.

In the case of the LT measured to predicted thrust stresses (see Figure 8), White and Layer's predictions for the low- and high-profile culverts were slightly unconservative (15 percent) for the low and medium plasticity clays, but very unconservative (30 percent) for the high plasticity clay. Conversely, the same structures were conservative by 15 percent for the low- and medium-plasticity clays and were within 2 percent for the high-plasticity clays by the AASHTO design. The LT response predicted by White and Layer, as well as the AASHTO code for the semicircular arch, was unconservative by 20 and 30 percent for the medium- and low-plasticity clays and by more than 50 percent for the very plastic clay.

The semicircular arch had the greatest wall thrust stresses of any structure for any soil because of its crown rising with time, which transferred soil load into the structure. As expected from the pore pressure measurements in the red clay [Figure 7(*b*)], definite positive arching occurred, which is reflected by its low thrust stresses compared to the other clays (Figure 8) for all structures.

TABLE 4 Ratio of Measured Axial Forces (EOC, LT) Versus White and Layer (WL) and AASHTO Code (AC) Values and Maximum Bending Moments for Shoulder of Culverts

Case	Struct.	Soil	EOC/WL	LT/WL	EOC/AC	LT/AC	Moment (m-kN/m)
1	low prof	orange	0.935	1.047	0.764	0.855	5311
2	low prof	red	0.923	1.015	0.754	0.829	6628
3	low prof	green	0.963	1.220	0.786	0.997	9643
4	semicirc	orange	1.187	1.305	1.187	1.305	10960
5	semicirc	red	0.848	1.198	0.848	1.198	14412
6	semicirc	green	1.019	1.510	1.019	1.510	17792*
7	high prof	orange	0.998	1.116	0.807	0.902	8994
8	high prof	red	0.831	1.038	0.672	0.840	11405
9	high prof	green	0.872	1.268	0.706	1.025	16048

* reached the yield value

The LT maximum bending moments for all nine cases are provided in Table 4. They are plotted in Figure 9(*a*) versus geometry and in Figure 9(*b*) as a function of soil plasticity (*PI*). *R* is the rise, *S* is the span and R_1/R_2 is the ratio of the culvert's top radius to its springline radius. All the values tabulated or plotted are for the thrust beam location because they were the maximum. Note the linear relationship among bending moment, culvert geometry, and soil plasticity. This latter correlation was expected because the soil's compressibility increases with liquid limit (which affects *PI*, see Table 1).

The semicircular arch had the highest moments (yielded in the case of the green clay), and the low profile had the smallest. Also, the medium plasticity soil, which had the lowest thrust stresses due to arching, had higher bending moments than the low plasticity soil because of its greater deflections due to its higher compressibility.

A comparison between EOC and long-term bending stresses are shown in Figure 5. The following expression may be used to estimate the long-term maximum bending moments given in Table 4:

$$M_b = (1.4 + .0633PI)(R/S)\sqrt{(Rs/Rt)}S^3 \text{ (soil unit wt)} \quad (1)$$

where

R = culvert height,
S = culvert span (width),
Rs = radius of curvature of the culvert side, and
Rt = radius of curvature of the culvert top.

The above expression is accurate to within 5 percent for all nine cases.

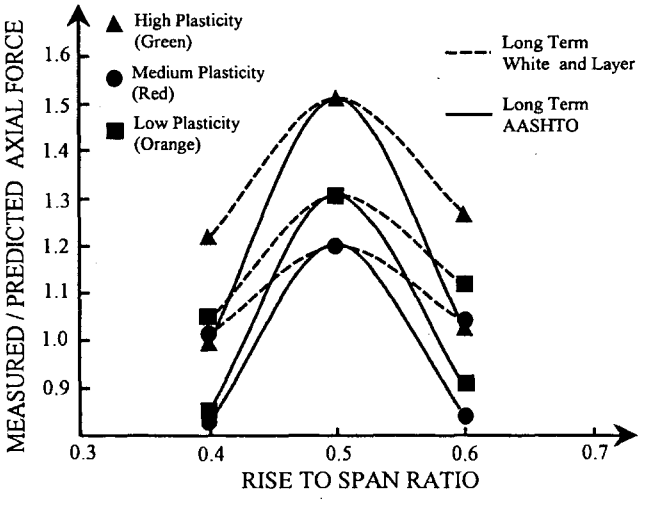

FIGURE 8 Ratio of measured to predicted axial thrust forces.

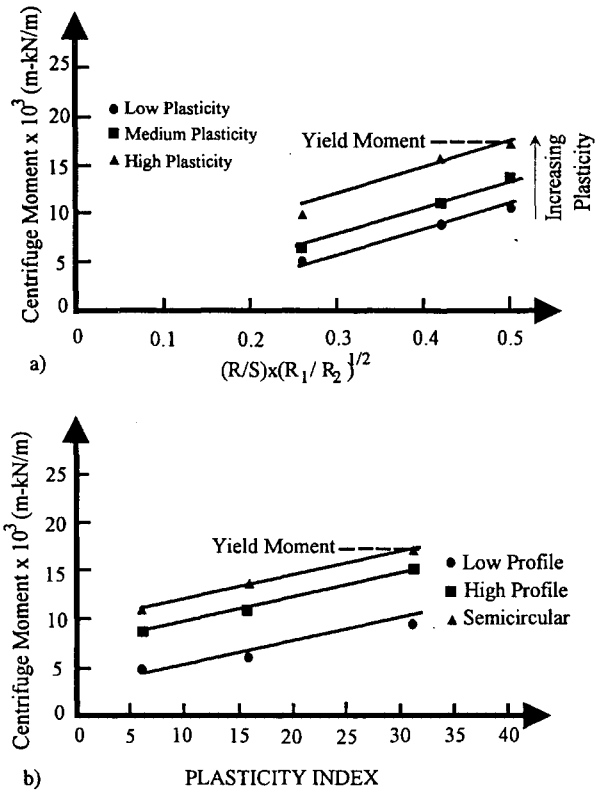

FIGURE 9 Long-term bending moments in the culverts' shoulders: (*a*) function of geometry; (*b*) function of soil plasticity.

CONCLUSIONS

The following results were concluded from this study:

- White and Layer's (*10*) method of determining wall stresses at the culvert's springline predicts very well EOC stresses when cohesive embankment soils are used. The AASHTO (*2*) code is slightly more conservative (25 to 30 percent) at the end of construction for the low- and high-profile culverts.
- The use of cohesive backfill has a definite adverse effect on the long-term response of the soil-culvert system. Maximum increases on the order of 50 percent for axial thrust and 100 percent for bending moments were observed.
- The culvert's initial shape has a significant influence on its long-term deflections and wall stresses (axial and bending).
- Because the semicircular arch has a single radius of curvature without a reentrant angle at its footing, it develops a deflected shape much different than that of the low- or high-profile arches. The long-term deflected pattern of the semicircular arch is inward at the shoulder and outward at the crown and springline (side) of the culvert, respectively. Both the low- and high-profile arches were outward everywhere except at the crown (top) of the culverts. Consequently, the mode of failure and the stresses in the semicircular versus low- and high-profile culverts are different.
- All culverts exhibited the maximum bending moment at their shoulders. The maximum moments were highest for the semicircular culvert, lower for the high-profile culvert, and lowest for the low-profile culvert. A linear relationship between maximum bending moment and plasticity index was measured (for a given culvert shape). A linear relationship also existed between maximum moment and the culvert's geometry (for a given plasticity index).
- The semicircular arch gave the greatest long-term thrust stress increase because its crown was rising (other shapes were subsiding) with time, which transferred more of the clay's overburden weight to the culvert. For a given shape, a unique relationship between soil plasticity and its axial thrust stresses did not exist. The AASHTO code (*2*) predicted conservatively (within 15 percent) the long-term axial thrust for all clays around the low- and high-profile culverts, whereas, White and Layer (*10*) predictions were 30 percent unconservative for the same structures. Both methods gave unconservative thrust stresses, 20 to 50 percent, depending on plasticity, for the semicircular arch.

Overall, the semicircular arch is not recommended when the other two shapes are available or without a reentrant angle (i.e., horseshoe culvert) at its footing in deep plastic clay backfills. Also, the designer should make every effort to use low-plasticity backfill which has high permeability and low compressibility.

Although the significance of soil type and geometry have been identified, the effects of backfill depths and the size of the granular zone around the culvert warrant further investigation before a design procedure may be established. The study should include LT wall stresses (bending and axial) as well as deformation and wall buckling. The centrifuge is an excellent means of conducting the study because of cost and the fact that the *G*-level squared speeds up the consolidation time.

ACKNOWLEDGMENTS

The support of the National Science Foundation is gratefully acknowledged. The authors also wish to express their appreciation to Habib Tabatabai and Phanio Cleanthous for their aid in constructing and recording the soil-culvert systems. Special thanks go to the reviewers, who improved the original text.

REFERENCES

1. Selig, E. T. Large Buried Metal Culvert Design and Construction. *Proc., 11th Ohio River Valley Soil Seminar on Earth Pressures and Retaining Structures*, Clarksville, Ind., 1980, pp. 13–22.
2. *Specifications—Bridges*, American Association of State Highway and Transportation Officials, Washington, D.C., 1989, pp. 186–188.
3. Scheer, A. C., and G. A. Willet. Rebuilt Wolf Creek Culvert Behavior. In *Highway Research Record 262*, HRB, Washington, D.C., 1969, pp. 1–10.
4. Culvert Failure Kills Five. *Engineering News Record*, Jan. 1983, p. 12.
5. Committee on Soil-Structure Interaction on Subsurface Conduits. Minutes. TRB, National Research Council, Washington, D.C., Jan. 1982.
6. McVay, M. C., and P. Papadopoulos. Long-Term Behavior of Buried Large-Span Culverts. *Journal of the Geotechnical Engineering Division*, ASCE, Vol. 112, No. GT4, Apr. 1986, pp. 424–442.
7. Avgherinos, P. J. *Centrifugal Testing of Models Made of Soil.* Ph.D. thesis. University of Cambridge, England, 1969.
8. Duncan, J. M., and B. R. Seed. Compaction-Induced Earth Pressures Under K_0-Conditions. *Journal of the Geotechnical Engineering Division*, ASCE, Vol. 112, No. 1, Jan. 1986, pp. 1–22.
9. Trollope, D. H., A. M. Aust, M. G. Speedie, and I. K. Lee. Pressure Measurements on Tallaroop Dam Culvert. *Proc., Fourth Australia-New Zealand Conference*, Sydney, Australia, 1963, pp. 169–184.
10. White, L. L., and J. P. Layer. The Corrugated Metal Conduit as a Compression Ring. *Proc., Highway Research Board*, Vol. 39, 1960, pp. 389–397.

Publication of this paper sponsored by Committee on Subsurface Soil-Structure Interaction.